Crackling to periodic dynamics in granular media

Aghil Abed Zadeh, Jonathan Barés, Robert Behringer

▶ **To cite this version:**

Aghil Abed Zadeh, Jonathan Barés, Robert Behringer. Crackling to periodic dynamics in granular media. Physical Review E , 2019, 99 (4), 10.1103/PhysRevE.99.040901 . hal-02115917

HAL Id: hal-02115917
https://hal.science/hal-02115917v1

Submitted on 30 Apr 2019

HAL is a multi-disciplinary open access archive for the deposit and dissemination of scientific research documents, whether they are published or not. The documents may come from teaching and research institutions in France or abroad, or from public or private research centers.

L'archive ouverte pluridisciplinaire **HAL**, est destinée au dépôt et à la diffusion de documents scientifiques de niveau recherche, publiés ou non, émanant des établissements d'enseignement et de recherche français ou étrangers, des laboratoires publics ou privés.

Crackling to periodic dynamics in granular media

Aghil Abed Zadeh,[1,*] Jonathan Barés,[1,2,†] and Robert P. Behringer[1]
[1]*Department of Physics & Center for Nonlinear and Complex Systems, Duke University, Durham, North Carolina 27708, USA*
[2]*Laboratoire de Mécanique et Génie Civil, Université de Montpellier, CNRS, Montpellier, France*

We study the local and global dynamics of sheared granular materials in a stick-slip experiment, using a slider and a spring. The system crackles, with intermittent slip avalanches, or exhibits irregular or periodic dynamics, depending on the shear rate and loading stiffness. The global force on the slider during shearing captures the transitions from the crackling to the periodic regime. We deduce a dynamic phase diagram as a function of the shear rate and the loading stiffness and associated scaling laws. Using photoelastic particles, we also capture the grain-scale stress evolution, and investigate the microscopic behavior in the different regimes.

I. INTRODUCTION

Sheared amorphous materials yield and flow, when sufficiently loaded [1–3]. The flow can be spatially heterogeneous and erratic in time. This intermittent behavior has been observed in phenomena as diverse as seismicity [4–6], fracture [7–9], damage [10,11], friction [12,13], plasticity [14,15], magnetization [16,17], wetting [18,19], neural activity [20,21], and granular avalanches [22–26].

In granular media, the intermittent dynamics, also called "crackling" [27], is associated with the transition between jammed and unjammed states [26,28] around yielding: When slowly sheared, a granular system may stick and slip, with slip sizes spanning a wide range of scales [29–32]. Meanwhile, under certain conditions, some sheared systems do not obey this crackling behavior. Instead, slips occur "periodically" with a narrow size distribution [33–36]. For other systems, the oscillations may be damped or the grains flow continuously. In addition to safety and industrial challenges to control these dynamics, understanding these different behaviors is crucial in granular physics and many other associated fields, exhibiting similar dynamics.

The crackling response of granular media is of particular interest [2,26,37] and the effect of the system's parameters on the dynamics, their scaling laws, and avalanche shapes has been investigated [38–41]. Other studies concentrated on understanding the transition between the periodic stick-slip and steady sliding regimes [36,42]. However, the transitions from crackling to periodic dynamics have not been studied. Consequently, fundamental issues remain: Do crackling and periodic dynamics arise from fundamentally different systemic behaviors, identifiable at a microscopic scale, or do they occur as bifurcations controlled by system-scale parameters? Are they the only dynamical regimes? What is the interplay between the grain-scale mechanics and the macroscopic system parameters?

The study reported here addresses these questions. Experiments on sheared granular materials reproduce crackling and periodic regimes, with an "irregular" regime in between. Adjusting the driving rate and the system stiffness causes the system to transition between different behaviors, and yields a dynamic phase diagram. The system observables, such as the loading force, are analyzed in both regimes. We find that the periodic behavior of the macroscopic force is accompanied by erratic microscopic stress dynamics and is observed only with finite loading stiffness.

II. EXPERIMENTS

The experimental device provides data both at the global and local scales, similarly to Refs. [36,43]. As shown in Fig. 1(a) [44], a stage pulls a two-dimensional (2D) frictional slider of fixed length 25 cm and variable mass M. The stage, which moves at constant speed c, pulls the slider by means of a linear spring of stiffness k, which represents the loading stiffness. The slider rests on a vertical bed of fixed depth $L = 9.5$ cm, and length 1.5 m consisting of bidisperse cylindrical photoelastic particles with diameters 0.4 and 0.5 cm (small/big ratio of 2.7) to avoid crystallization. Unless specified, the experiments are made with a slider of mass $M =$ 85 g. The slider+particles system is sandwiched between two dry-lubricated glass plates. The slider bottom is toothed to enhance the friction with the grains. The force f applied to the spring is measured by a sensor at a frequency of 1 kHz. The system is designed to be at a constant pressure, and the slider can move in either the horizontal or vertical directions. However, the granular bed is prepared flat enough that it stays mostly horizontal, while being pulled. Due to a free granular surface, a small pile of granular matter develops in front of the slider. The front of the slider is designed with an angle and without teeth to reduce the force applied by the pile. We also prepare the initial front pile the same as the steady state such that the dynamics is stationary. The system is lit from behind by a polarized light source. In front, a camera with a crossed polarizer images the grains and slider at a frequency of 120 Hz [see Fig. 1(b)]. The photoelastic response of the

*aghil.abed.zadeh@duke.edu
†jb@jonathan-bares.eu

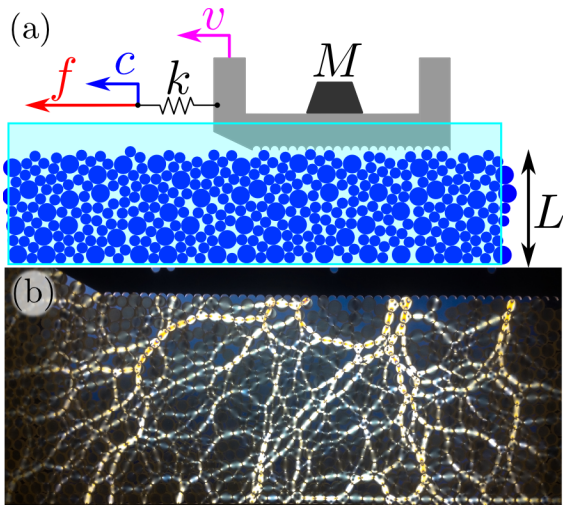

FIG. 1. (a) Sketch of the experiment from the side: A slider is pulled over a 2D vertical granular bed of bidisperse photoelastic disks. The slider is pulled at a constant speed c by means of a spring of stiffness k. The pulling force f is measured by a force sensor, connected to the spring. The system is lit from behind by polarized light and observed from the front by a fast (120 fps) camera equipped with a crossed polarizer. (b) Photoelastic response of the granular bed during loading.

media provides a local measure of the stress from the image intensity I [29]. We analyze the mean response of the granular medium as the fast imaging is not accurate enough to provide grain-level stress measurement.

III. RESULTS

Figure 2 shows the evolution of the pulling force $f(t)$ (colored) and of the slider speed $v(t)$ (black) for three typical c's. At low speed [Fig. 2(a)], $c = 0.1$ mm/s, the system crackles [27,43]. The slider is immobile most of the time, as it loads up elastically. It then undergoes erratic sudden jumps. These unloading events are accompanied by slider slips and irreversible grain flows. At high speed [Fig. 2(c)], $c = 100$ mm/s, the slider never stops, and exhibits smooth periodic oscillations. In between [Fig. 2(b)], $c = 15$ mm/s, most of the time, the slider exhibits slow noisy displacements with irregular jumps, smoother and less intense than in the crackling case. Figure 2(d) shows the power spectral density (PSD) of the force signal $\mathcal{P}_f$ for these three different cases. At low c, above a flat lower cutoff, $\mathcal{P}_f$ follows a power law spanning more than two decades in ω with an exponent -2.4 ± 0.2, similar to Brownian noise [45]. At a medium c, $\mathcal{P}_f$ is constant for a large range of ω, such as white noise, and decays rapidly above a cutoff frequency ($\approx$10 Hz). For higher c, $\mathcal{P}_f$ develops a peak with a characteristic frequency which depends on c, and differs from the constant inertial frequency of the system, $\omega_{\text{syst}} = \frac{1}{2\pi}\sqrt{\frac{k}{M}} = 4.6$ Hz.

The system can transit from the *crackling* to *irregular* to *periodic*. Figure 3(a) shows the evolution of $\mathcal{P}_f$, as c varies, for fixed k [44]. Considering the crackling regime (small c) and ignoring the flat part of the PSD at high frequencies (related to the medium damping), $\mathcal{P}_f$ is fitted to

$$\mathcal{P}_f(\omega) \propto (1 + \omega/\omega_{\text{min}})^{-\beta} e^{-\omega/\omega_{\text{max}}},$$

where ω_{min} and ω_{max} are the lower and upper power-law cutoffs, respectively, and $\beta = 2.4 \pm 0.2$. The number of decades for which $\mathcal{P}_f$ obeys a power law $\log_{10}(\omega_{\text{max}}/\omega_{\text{min}})$ decreases as c increases. This is quantified in the inset of Fig. 3(b), showing that this number is roughly inversely proportional to c: $\omega_{\text{max}}/\omega_{\text{min}} \propto 1/c$. Moreover, in the inset of Fig. 3(a), $\mathcal{P}_f$ curves, except for their upper cutoffs, collapse when ω is scaled by c. This implies that $\omega_{\text{min}} = \kappa c$, where $\kappa \approx 10^2$ (1/m) is a characteristic wave number of the system, and independent of c. For higher c, a bump appears close to ω_{min}.

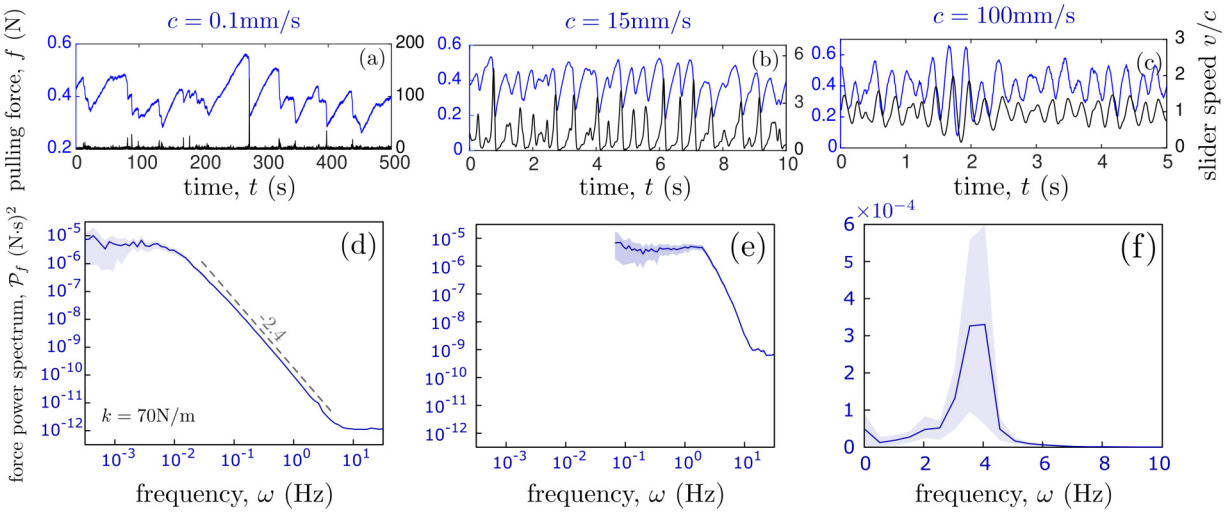

FIG. 2. Typical signals. Evolution of the slider speed $v(t)$ (black, lower) and pulling force $f(t)$ (colored, upper) for different loading speeds ($c = 0.1$, 15, and 100 mm/s) displaying different dynamics: (a) Crackling at low speed, (b) irregular at medium speed, and (c) periodic at high speed. (d)–(f) Corresponding power spectral density of the force signal $\mathcal{P}_f$. A dashed line shows a slope corresponding with the exponent -2.4 ± 0.2 fitted on the power law obtained for $c = 0.1$ mm/s. The shaded areas show the 95% confidence interval of the curves. (d) and (e) are in log-log scale, while (f) is in linear scale. Experiments are carried out with a spring of stiffness $k = 70$ N/m.

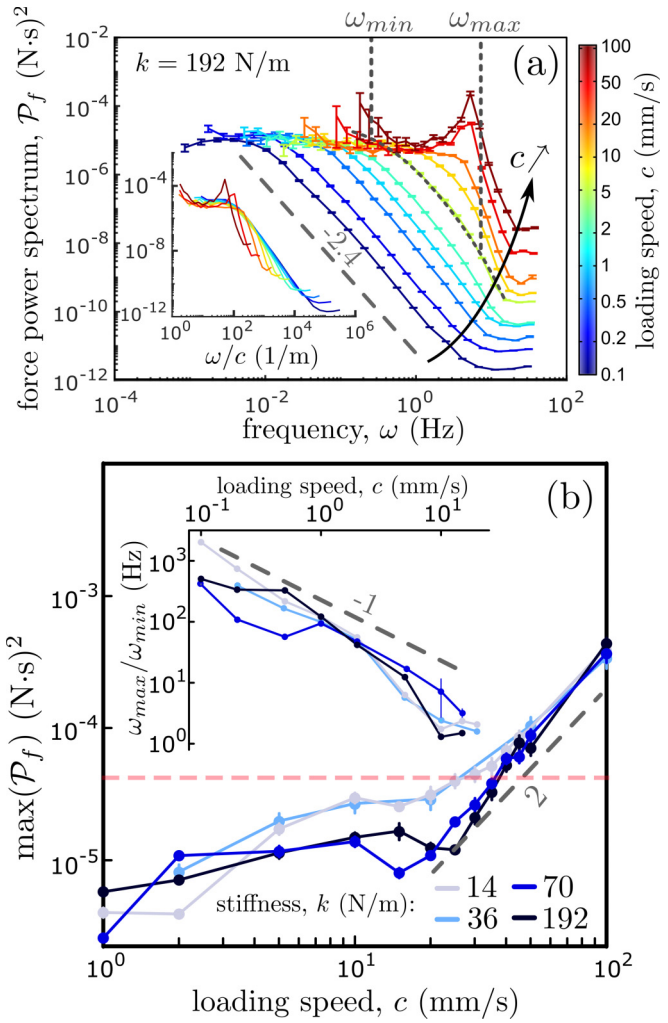

FIG. 3. (a) Force power spectra $\mathcal{P}_f(\omega)$ for different loading speeds, $c \in [0.1, 100]$ mm/s with $k = 192$ N/m. For $c = 2$ mm/s, $\mathcal{P}_f$ is fitted by a gamma function displayed by a dashed line with lower ($\omega_{\min}$) and upper ($\omega_{\max}$) cutoff positions. A straight dashed line shows a slope corresponding with the exponent -2.4 fitted to the lowest c curve. Inset: $\mathcal{P}_f$ with frequency scaled by c. (b) Maximum of $\mathcal{P}_f$ as a function of c, for power spectra with a bump. The red horizontal line represents the threshold used to define the periodic regime in Fig. 4. A dashed line with slope 2 is given to guide the eye. Inset: Spreading of the power-law regime (if any) $\omega_{\max}/\omega_{\min}$ as a function of c. A dashed line with slope -1 is given to guide the eye. Different curves correspond to different k.

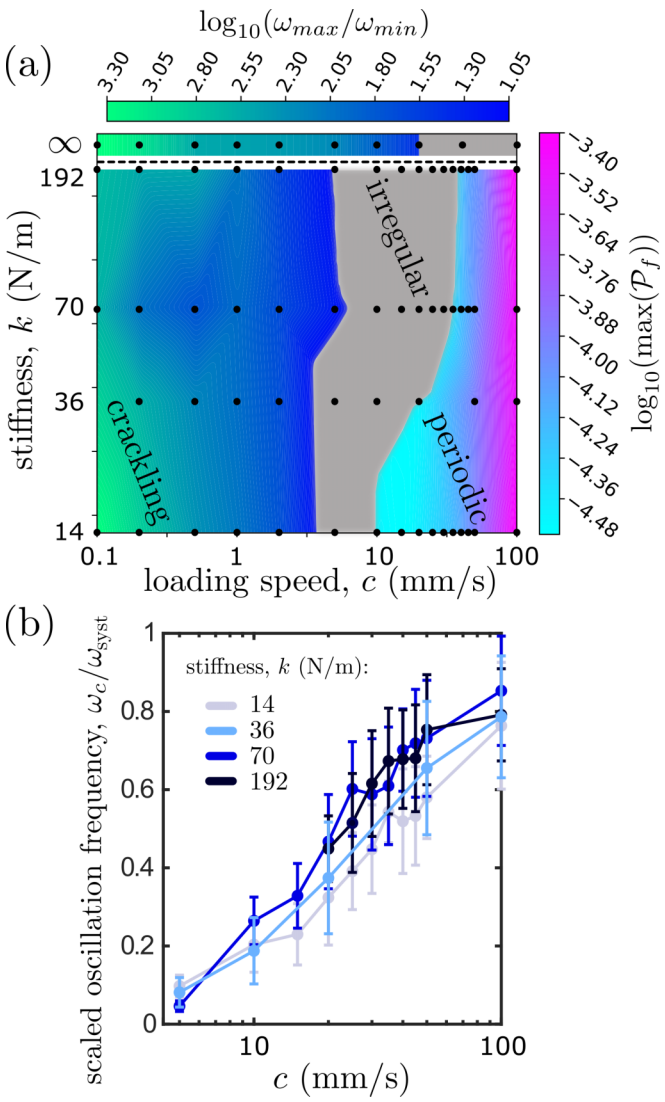

FIG. 4. (a) Dynamic phase diagram as a function of k and c. The color plot of the crackling regime uses the color bar on the top. It shows the PSD power-law range $\log_{10}(\omega_{\max}/\omega_{\min})$ (when larger than 1). The color plot of the periodic regime uses the color bar on the right. It is a map of the maximum of $\mathcal{P}_f$, when larger than $10^{-4.6}$ (N s)^2. The irregular region, shown in gray, is the complementary. Its complex boundary geometries encompass the measurement uncertainty. Black dots are experimental measurement points, and the rest of the map is linearly interpolated (in the log space). The top line shows $k = \infty$, as the slider is pulled with a chain. (b) Evolution of PSD peak frequency, ω_c in the periodic regime, scaled by ω_{syst}, vs c on log-linear scales. The scaling collapses the curves for different stiffnesses within the error bars. The error bars represent the width of the peaks in power spectra.

This indicates the onset of oscillations at a frequency ω_c. The inset of Fig. 3(a) shows that, unlike $\omega_{\min}$, ω_c does not scale with c, since the peaks do not collapse. Figure 3(b) shows the value of $\mathcal{P}_f$ at the peak. This scaling quantifies the oscillation strength.

Figure 4(a) presents the phase diagram that quantifies crackling and periodicity as a function of c and k. The behavior is classified as crackling when there is a full decade or more of power-law decay [$\log_{10}(\omega_{\max}/\omega_{\min}) > 1$], a commonly accepted definition [46,47]. Conversely, the value of $\mathcal{P}_f$ at the peak is higher for higher c. In the domain where $\mathcal{P}_f > 10^{-4.6}$ (N s)^2 is above the low-frequency plateau, the periodic regime lies. Between these regions lies the irregular regime, where there is neither a clearly defined power-law span nor a well-defined spectral peak, but a white-noise PSD. Moreover, our experimental precision does not provide a clear critical c between crackling and periodic regimes. Figure 4(b) shows how the oscillation frequency evolves with c for different k's. We observe a vanishing frequency and consequently a diverging period near the transition. This relation along with the fast and slow processes in stick-slip dynamics is

reminiscent of a homoclinic bifurcation with c [48] as the bifurcation parameter. Moreover, the dependence of frequency on c shows that the periodicity is not trivially induced by loading stiffness or can be described by a simple one-dimensional (1D) frictional model [44], and the granularity of medium plays a crucial role in the dynamics. This relation might be due to the interplay of granular dilation with speed and the effective friction [33]. Furthermore, the curves for different stiffnesses approximately collapse, within the experimental uncertainty, when ω_c is scaled by $\omega_{\text{syst}} = \frac{1}{2\pi}\sqrt{\frac{k}{M}}$ [44].

We also investigate the force signal probability distribution function (PDF) $P(f)$. Figure 5(a) shows $P(f)$ for different c's, and fixed k. Regardless of the shear rate, these PDFs are well fitted by a Gaussian function of standard deviation $\sigma(c, k)$. Their mean value is independent of c in the range of speeds explored here. Similarly, as shown in the upper inset of Fig. 5(a), the force fluctuations, quantified by σ, remain constant [$\sigma \approx 0.065$ (N)] in the crackling and irregular regimes. However, σ starts to increase when the periodic behavior is first observed (from $c \approx 20$ mm/s), accompanied by the decoupling of the spring force and the granular friction force on the slider. This broadening is most likely due to the smooth turning points in the force curve for the periodic system, which imply that more time is spent at the extreme values of the force than in the crackling regime.

We also explore the effect of other macroscopic parameters. Unlike previous findings [39], changing the granular layer depth L does not change the system's behavior [44] to our experimental precision. The slider motion creates a narrow shear band, and particle flow is limited to the few top layers of grains. The narrowness of this shear band, where plastic granular flow occurs, is likely responsible for the fact that L does not play a significant role in our experiment. However, the granular global pressure, from the slider weight $W = Mg$, changes $P(f)$ significantly. The lower inset of Fig. 5(a) shows these PDFs when the force is scaled by the slider mass f/W. $P(f/W)$ for different M collapse on a single curve, indicating that M controls both the mean and fluctuations of f [44]. This collapse also implies a linear relation between the global pressure $\mathcal{P}$ and the mean global shear stress τ and its fluctuations σ_τ. This provides a constant average friction coefficient, $\mu = \bar{\tau}/\mathcal{P} \approx 0.47$, for the slowly sheared medium.

We also study the relation between the global dynamics, as characterized by the $f(t)$, and the aggregated local dynamics determined by the granular stress. The aggregated local stress is computed from the polarized images' mean intensity I [44], in a region which covers all granular layers and is $\sim$1.5 slider's length wide to include all force evolution. Figure 5(b) shows the image intensity PSD, $\mathcal{P}_I$, for several c's at fixed $k = 70$ N/m. As $\mathcal{P}_f$ in the crackling regime, $\mathcal{P}_I$ follows a power law with an exponent -2.2 ± 0.2, and the frequency interval of this power-law regime decreases as c increases. However, as c increases, we do not observe a clear peak in $\mathcal{P}_I$ that would indicate a periodic regime. For high c, we observe much faster stress fluctuations in the granular medium, compared to the slider dynamics [44]. The high stiffness and low inertia of particles may induce this difference. In this case, we observe a decoupling between the granular medium mean stress and the mean flow of particles, which is correlated with the slider motion. These erratic stress fluctuations show

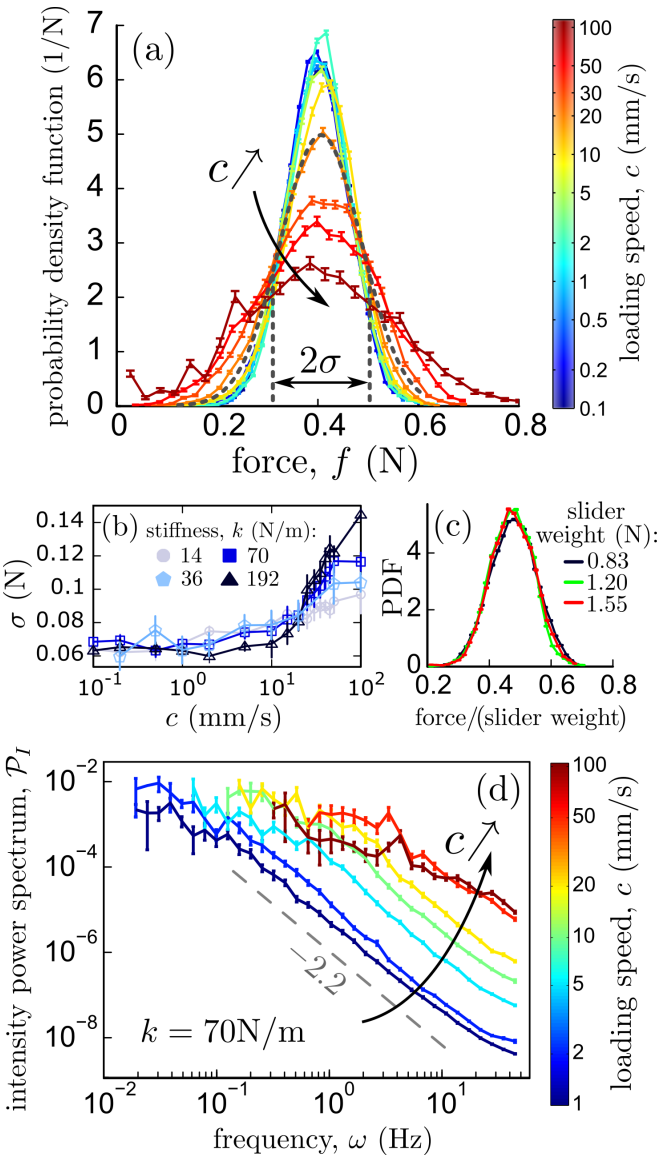

FIG. 5. (a) Probability density function of force $P(f)$, for different loading speeds c, at fixed stiffness $k = 192$ N/m. For $c = 20$ mm/s, $P(f)$ is fitted by a Gaussian displayed by a dashed line. The standard deviation is σ. (b) σ vs c for different stiffnesses, $k \in \{14, 30, 70, 192\}$ N/m. (c) PDF of the force signal scaled by the slider weight for different weights, $Mg \in \{0.83, 1.2, 1.55\}$ N, with $c = 0.5$ mm/s and $k = 192$ N/m. (d) Image intensity $[I(t)]$ power spectra $\mathcal{P}_I(\omega)$ for different $c \in [1, 100]$ mm/s with $k = 70$ N/m. A straight dashed line shows a slope corresponding with the exponent -2.2 ± 0.2 fitted to the lowest speed.

a nonperiodic friction force on the slider, moving periodically. This granular boundary friction force, when coupled with finite loading stiffness [44] and the slider's inertia, results in periodic oscillations at the macroscopic scale.

IV. CONCLUDING DISCUSSION

The experiments reported here demonstrate crackling, irregular, and periodic dynamics while shearing granular matter via a slider and a spring. The system behavior depends on

the stage speed c and the loading stiffness k. The transitions between regimes occur over regions of $c - k$ space, without sharp crossovers. The other main observations of these experiments are as follows: (i) The shearing force PSD provides a useful tool to indicate the dynamics of the system for a given set of system control parameters, namely, loading speed, system stiffness, global pressure, and system size. (ii) The transition to a periodic regime shows a diverging period, which is similar to a homoclinic bifurcation, where c is the primary control parameter. (iii) The shearing force PDF follows a Gaussian distribution with an increasing standard deviation in the periodic regime. (iv) No periodic behavior is observed for the local stress dynamics, which implies the important role of the stiffness and inertia of the loading boundary in the periodic regime.

These observations are in agreement with various numerical simulations. Lacombe *et al.* [42] introduced a simple friction model, similar to our experiment, with two degrees of freedom, considering dilation. They reproduced stick-slip, inertial oscillations and sliding regimes by increasing the shear rate. However, no crackling dynamics was observed, since their model lacks stochasticity. Our phase diagram, presented in Fig. 4, may be a detailed version of the stick-slip domain of their diagram. In an experimental study, Kaproth *et al.* [35] observed only periodic stick-slip and sliding regimes, and the driving rate only affects the slip event period. We believe they do not observe crackling dynamics because of the monodispersity of their granular layers. In other studies, Aharonov *et al.* [38] simulated a system, very similar to ours, using the discrete element method. They also observed crackling, oscillatory, and sliding regimes by changing the loading speed and the slider mass. However, the effect of the stiffness was not tested and the exact domains of the crackling regime were not investigated. Liu *et al.* [39] also studied the effect of the driving rate on avalanches. As in our experiments, they observed that increasing the driving rate decreases the power-law range of the avalanche size distribution, i.e., the number of decades over which the avalanche size PDF obeys a power law. Avalanches have also been observed in depinning models and a phase diagram of dynamical regimes for such a model has been demonstrated [49] as a function of c, k, and L.

The findings of this Rapid Communication can inform a number of open problems in other fields, such as avalanche dynamics for nonzero driving rate in crackling systems and depinning transitions, and fluctuating dynamics of amorphous media, including seismicity. Future work is required to investigate global and local (space-time) avalanche statistics.

ACKNOWLEDGMENTS

We would like to acknowledge Josh Socolar, Mark Robbins, and Sid Nagel for their helpful conversations and funding support from NSF-DMR1206351, NASA NNX15AD38G, The William M. Keck Foundation, and DARPA Grant No. 4-34728.

[1] I. Regev, J. Weber, C. Reichhardt, K. A. Dahmen, and T. Lookman, Reversibility and criticality in amorphous solids, Nat. Commun. **6**, 8805 (2015).

[2] J. Lin, T. Gueudré, A. Rosso, and M. Wyart, Criticality in the Approach to Failure in Amorphous Solids, Phys. Rev. Lett. **115**, 168001 (2015).

[3] C. E. Maloney and A. Lemaître, Amorphous systems in athermal, quasistatic shear, Phys. Rev. E **74**, 016118 (2006).

[4] P. Bak, K. Christensen, L. Danon, and T. Scanlon, Unified Scaling Law for Earthquakes, Phys. Rev. Lett. **88**, 178501 (2002).

[5] J. Davidsen and G. Kwiatek, Earthquake Interevent Time Distribution for Induced Micro-, Nano-, and Picoseismicity, Phys. Rev. Lett. **110**, 068501 (2013).

[6] J. Barés, A. Dubois, L. Hattali, D. Dalmas, and D. Bonamy, Aftershock sequences and seismic-like organization of acoustic events produced by a single propagating crack, Nat. Commun. **9**, 1253 (2018).

[7] M. J. Alava, P. K. V. V. Nukala, and S. Zapperi, Statistical models of fracture, Adv. Phys. **55**, 349 (2006).

[8] D. Bonamy, S. Santucci, and L. Ponson, Crackling Dynamics in Material Failure as the Signature of a Self-Organized Dynamic Phase Transition, Phys. Rev. Lett. **101**, 045501 (2008).

[9] J. Barés, M. L. Hattali, D. Dalmas, and D. Bonamy, Fluctuations of Global Energy Release and Crackling in Nominally Brittle Heterogeneous Fracture, Phys. Rev. Lett. **113**, 264301 (2014).

[10] A. Petri, G. Paparo, A. Vespignani, A. Alippi, and M. Costantini, Experimental Evidence for Critical Dynamics in Microfracturing Processes, Phys. Rev. Lett. **73**, 3423 (1994).

[11] H. V. Ribeiro, L. S. Costa, L. G. A. Alves, P. A. Santoro, S. Picoli, E. K. Lenzi, and R. S. Mendes, Analogies Between the Cracking Noise of Ethanol-Dampened Charcoal and Earthquakes, Phys. Rev. Lett. **115**, 025503 (2015).

[12] W. F. Brace and J. D. Byerlee, Stick-slip as a mechanism for earthquakes, Science **153**, 990 (1966).

[13] P. A. Johnson, H. Savage, M. Knuth, J. Gomberg, and C. Marone, Effects of acoustic waves on stick–slip in granular media and implications for earthquakes, Nature (London) **451**, 57 (2008).

[14] S. Zapperi, A. Vespignani, and H. E. Stanley, Plasticity and avalanche behaviour in microfracturing phenomena, Nature (London) **388**, 658 (1997).

[15] S. Papanikolaou, D. M. Dimiduk, W. Choi, J. P. Sethna, M. D. Uchic, C. F. Woodward, and S. Zapperi, Quasi-periodic events in crystal plasticity and the self-organized avalanche oscillator, Nature (London) **490**, 517 (2012).

[16] J. S. Urbach, R. C. Madison, and J. T. Markert, Interface Depinning, Self-Organized Criticality, and the Barkhausen Effect, Phys. Rev. Lett. **75**, 276 (1995).

[17] G. Durin and S. Zapperi, The Barkhausen effect, in *The Science of Hysteresis*, edited by G. Bertotto and I. Mayergoyz (Academic, New York, 2005), p. 181.

[18] D. Ertaş and M. Kardar, Critical dynamics of contact line depinning, Phys. Rev. E **49**, R2532 (1994).

[19] R. Planet, S. Santucci, and J. Ortín, Avalanches and Non-Gaussian Fluctuations of the Global Velocity of Imbibition Fronts, Phys. Rev. Lett. **102**, 094502 (2009).
[20] J. M. Beggs and D. Plenz, Neuronal avalanches in neocortical circuits, J. Neurosci. **23**, 11167 (2003).
[21] T. Bellay, A. Klaus, S. Seshadri, and D. Plenz, Irregular spiking of pyramidal neurons organizes as scale-invariant neuronal avalanches in the awake state, Elife **4**, e07224 (2015).
[22] B. Miller, C. C. O'Hern, and R. P. Behringer, Stress Fluctuations for Continuously Sheared Granular Materials, Phys. Rev. Lett. **77**, 3110 (1996).
[23] N. W. Hayman, L. Ducloué, K. L. Foco, and K. E. Daniels, Granular controls on periodicity of stick-slip events: Kinematics and force-chains in an experimental fault, Pure Appl. Geophys. **168**, 2239 (2011).
[24] S. P. Pudasaini and K. Hutter, *Avalanche Dynamics: Dynamics of Rapid Flows of Dense Granular Avalanches* (Springer, Berlin, 2007).
[25] A. Le Bouil, A. Amon, S. McNamara, and J. Crassous, Emergence of Cooperativity in Plasticity of Soft Glassy Materials, Phys. Rev. Lett. **112**, 246001 (2014).
[26] J. Barés, D. Wang, D. Wang, T. Bertrand, C. S. O'Hern, and R. P. Behringer, Local and global avalanches in a two-dimensional sheared granular medium, Phys. Rev. E **96**, 052902 (2017).
[27] J. P. Sethna, K. A. Dahmen, and C. R. Myers, Crackling noise, Nature (London) **410**, 242 (2001).
[28] D. Bi, J. Zhang, B. Chakraborty, and R. P. Behringer, Jamming by shear, Nature (London) **480**, 355 (2011).
[29] D. Howell, R. P. Behringer, and C. Veje, Stress Fluctuations in a 2D Granular Couette Experiment: A Continuous Transition, Phys. Rev. Lett. **82**, 5241 (1999).
[30] I. Albert, P. Tegzes, R. Albert, J. G. Sample, A.-L. Barabási, T. Vicsek, B. Kahng, and P. Schiffer, Stick-slip fluctuations in granular drag, Phys. Rev. E **64**, 031307 (2001).
[31] A. Petri, A. Baldassarri, F. Dalton, G. Pontuale, L. Pietronero, and S. Zapperi, Stochastic dynamics of a sheared granular medium, Eur. Phys. J. B **64**, 531 (2008).
[32] S. Lherminier, R. Planet, G. Simon, K. J. Måløy, L. Vanel, and O. Ramos, A granular experiment approach to earthquakes, Rev. Cubana Fis. **33**, 55 (2016).
[33] S. Nasuno, A. Kudrolli, A. Bak, and J. P. Gollub, Time-resolved studies of stick-slip friction in sheared granular layers, Phys. Rev. E **58**, 2161 (1998).
[34] S. Nasuno, A. Kudrolli, and J. P. Gollub, Friction in Granular Layers: Hysteresis and Precursors, Phys. Rev. Lett. **79**, 949 (1997).
[35] B. M. Kaproth and C. Marone, Slow earthquakes, preseismic velocity changes, and the origin of slow frictional stick-slip, Science **341**, 1229 (2013).
[36] J. Krim, P. Yu, and R. P. Behringer, Stick–slip and the transition to steady sliding in a 2D granular medium and a fixed particle lattice, Pure Appl. Geophys. **168**, 2259 (2011).
[37] K. A. Dahmen, Y. Ben-Zion, and J. T. Uhl, A simple analytic theory for the statistics of avalanches in sheared granular materials, Nat. Phys. **7**, 554 (2011).
[38] E. Aharonov and D. Sparks, Stick-slip motion in simulated granular layers, J. Geophys. Res. **109**, B09306 (2004).
[39] C. Liu, E. E. Ferrero, F. Puosi, J.-L. Barrat, and K. Martens, Driving Rate Dependence of Avalanche Statistics and Shapes at the Yielding Transition, Phys. Rev. Lett. **116**, 065501 (2016).
[40] R. A. White and K. A. Dahmen, Driving Rate Effects on Crackling Noise, Phys. Rev. Lett. **91**, 085702 (2003).
[41] B. Luan and M. O. Robbins, Effect of Inertia and Elasticity on Stick-Slip Motion, Phys. Rev. Lett. **93**, 036105 (2004).
[42] F. Lacombe, S. Zapperi, and H. J. Herrmann, Dilatancy and friction in sheared granular media, Eur. Phys. J. E **2**, 181 (2000).
[43] A. Abed Zadeh, J. Barés, and R. P. Behringer, Avalanches in a granular stick-slip experiment: detection using wavelets, EPJ Web Conf. **140**, 03038 (2017).
[44] See Supplemental Material at http://link.aps.org/supplemental/10.1103/PhysRevE.99.040901 for more information including a full picture of the experiment, PSD of other k values, scaling curves of oscillation period, $\mathcal{P}_f$ and $P(f)$ for different L, $f(t)$ and $I(t)$ signals for different loading speeds and their relation, and a simple one-dimensional (1D) model.
[45] A. Baldassarri, F. Dalton, A. Petri, S. Zapperi, G. Pontuale, and L. Pietronero, Brownian Forces in Sheared Granular Matter, Phys. Rev. Lett. **96**, 118002 (2006).
[46] M. L. Goldstein, S. A. Morris, and G. G. Yen, Problems with fitting to the power-law distribution, Eur. Phys. J. B **41**, 255 (2004).
[47] A. Clauset, C. R. Shalizi, and M. E. J. Newman, Power-law distributions in empirical data, SIAM Rev. **51**, 661 (2009).
[48] S. H. Strogatz, *Nonlinear Dynamics and Chaos: With Applications to Physics, Biology, Chemistry, and Engineering* (Westview Press, Boulder, CO, 2015).
[49] J. Barés, L. Barbier, and D. Bonamy, Crackling Versus Continuumlike Dynamics in Brittle Failure, Phys. Rev. Lett. **111**, 054301 (2013).